Surface Science xxx (2015) xxx–xxx

Contents lists available at ScienceDirect

Surface Science

journal homepage: www.elsevier.com/locate/susc

The oxidation and surface speciation of indium and indium oxides exposed to atmospheric oxidants

Zachary M. Detweiler [1], Steven M. Wulfsberg [1], Matthew G. Frith, Andrew B. Bocarsly, Steven L. Bernasek *

Department of Chemistry, Princeton University, Princeton, NJ 08544, USA

ARTICLE INFO

Available online xxxx

Keywords:
Surface oxidation
Indium oxide
Water adsorption

ABSTRACT

Metallic indium and its oxides are useful in electronics applications, in transparent conducting electrodes, as well as in electrocatalytic applications. In order to understand more fully the speciation of the indium and oxygen composition of the indium surface exposed to atmospheric oxidants, XPS, HREELS, and TPD were used to study the indium surface exposed to water, oxygen, and carbon dioxide. Clean In and authentic samples of In_2O_3 and $In(OH)_3$ were examined with XPS to provide standard spectra. Indium was exposed to O_2 and H_2O, and the ratio of O^{2-} to OH^- in the O1s XPS region was used to monitor oxidation and speciation of the surface. HREELS and TPD indicate that water dissociates on the indium surface even at low temperature, and that In_2O_3 forms at higher temperatures. Initially, OH^- is the major species at the surface. Pure In_2O_3 is also OH^- terminated following water exposure. Ambient pressure XPS studies of water exposure to these surfaces suggest that high water pressures tend to passivate the surface, inhibiting extensive oxide formation.

1. Introduction

Indium in its pure elemental form is used in a few applications, such as a gasket seal in vacuum systems, as a heat conductor in electronic cooling and cryogenic applications, and as a reducing agent in chemical reactions [1–3]. More commonly, indium is either alloyed with other metals to modify their properties (for instance, as a component in eutectics like gallium–indium, gallium–indium–tin, and bismuth–indium–tin), combined with group V elements to make III–V semiconductors, or employed as a transparent conductor as indium oxide or, most often, indium tin oxide (ITO) [1]. In spite of these important uses, the ambient corrosion of indium metal and its oxides is not as well documented as more abundant and more widely used structural metals.

Due to its wide use in electronics, ITO, unlike In^0 and In_2O_3, has been characterized extensively using UHV techniques, but the attribution of oxide and hydroxide species (which are extremely important for performance and reproducibility) to Sn or In in ITO species is difficult and often ambiguous [4]. The work function of ITO can be altered by the method and parameters of preparation and a major contributor to this variation in properties is likely humidity [5,6]. SnO_2 nanoparticles have even been used as humidity sensors, showing significant conductivity perturbation in the presence of varying water vapor pressures [7]. Little attention has been placed on the role of In_2O_3–water interactions and essentially no studies have been done to discern the impact of atmospheric water on the speciation at the indium solid–gas interface. Elucidating the behavior of water at the gas–solid interface of indium is critical for future applications of indium metal and indium oxide, in addition to various indium containing mixed metal compounds. To determine the role of the indium oxidation state in aqueous electrochemical CO_2 reduction to formate, a deeper understanding of the interfacial speciation at the electrode surface was necessary. Recently the role of these specific oxides has been implicated in electrocatalytic CO_2 reduction at the oxidized indium electrode [8].

The study of metal and metal oxide interactions with small molecules is a well-developed field with many tools and techniques available. The study of oxygen and water corrosion of various structural metals is extensive, as is the case with the corrosion of iron, for example [9,10]. Some corrosion studies of indium metal have previously been performed. Lin et al. studied indium metal and indium (III) oxide using X-ray photoelectron spectroscopy (XPS) and Auger electron spectroscopy (AES) [11]. Rossnagel et al. employed AES to monitor the oxidation of In^0 with O_2, H_2O, CO, and CO_2, finding that an In oxide layer developed on exposure to all of the oxygen containing species, but in the case of CO and CO_2, oxidation may have been due to trace O_2 and H_2O contamination [12]. The oxidation of polycrystalline In^0 with O_2 was investigated with XPS and secondary ion mass spectrometry (SIMS) by Hewitt et al., who observed that O_2 continues to oxidize In^0 after thousands of Langmuirs (L) of O_2 exposure, forming an In_2O_3 film [13]. Concurrently, Sen et al. showed the formation of an In_2O_3 film on O_2 exposure to In^0, using AES. They noted the loss of In^0 signal after 10^6 L of O_2 exposure [14]. More recently, Jeong et al. studied the conductivity of indium oxide thin films as a function of deposition parameters including substrate temperature, deposition rate, and oxygen partial pressure, among others, and demonstrated the importance of the In/O ratio for the conductivity of the oxide film [15].

* Corresponding author.
[1] These authors contributed equally to the work described here.

http://dx.doi.org/10.1016/j.susc.2015.10.026
0039-6028/

It is important to note that these experiments on the detailed origin of oxygen and indium species were performed on UHV prepared samples, which qualitatively demonstrate significant differences from indium oxide species that are present after exposure to atmospheric conditions. Most notably, the identification of the high binding energy O 1s species observed in XPS measurements in all these experiments is conflicting. Here we attempt to address this shortcoming in the literature through a series of XPS, high-resolution electron energy loss spectroscopy (HREELS) and temperature programmed desorption (TPD) experiments. The explicit interactions of water with In^0 and In_2O_3 have not been characterized in terms of adsorption and dissociation, and the actual species formed at the solid–gas interface upon adsorption have been addressed only sparingly. Due to the lack of adequate information about these interactions and the role that indium speciation can play in the electronic properties of indium containing materials, the oxidation of indium upon exposure to H_2O, O_2, and CO_2 was systematically probed here.

2. Experimental

In order to probe the fundamental interactions of small molecule oxidants with the most common oxidation states of indium (metallic and trivalent), experiments were performed under both UHV and ambient pressure conditions. First, standards were measured as points of reference for the subsequent exposure studies.

2.1. Standard indium sample analysis

XPS control and dosing studies were performed using a VG Scientific Mk II ESCALab with a magnesium X-ray source and hemispherical electron analyzer set at 20 eV pass energy. Spectra were calibrated to the adventitious C 1s peak at 285 eV, or, when absent, the O 1s peak at 530 eV binding energy. Indium metal shot (Alfa Aesar 99.99% metals basis) was pounded into a flat circle of ~1.5 cm diameter and ~0.3 mm thickness and allowed to oxidize in atmosphere overnight before being introduced into vacuum. Powder samples of In_2O_3 (Aldrich 99.99% metals basis) and $In(OH)_3$ (Aldrich 99.99% metals basis) were liberally pressed onto carbon tape and introduced into vacuum as received. Clean metallic indium spectra were obtained by sputtering the native oxide sample with a differentially pumped Ar^+ beam at 2 keV and 10 mA emission current, delivering 4–6 μA to the sample for 1 h.

All XPS spectra were deconvoluted using CasaXPS peak fitting software with Shirley background subtractions and Gaussian–Lorentzian peak distributions.

2.2. Adsorption experiments studied via XPS

After obtaining the reference speciation peak information from standard samples, the progress of oxidation as a function of oxidant exposure was observed. H_2O, O_2, and CO_2 dosing experiments were performed on an Ar^+ sputtered indium metal substrate in the ESCAlab described above. The substrate was exposed by controllably leaking in the respective oxidants from between 0.5 L and 10^5 L at pressures from 10^{-9} to 10^{-5} Torr and recording In 3d, In Auger, O 1s, C 1s and survey XPS and Auger spectra after each exposure.

Ultra-high purity O_2 and CO_2 were obtained from AirGas Inc. and leaked into the chamber through a mechanically pumped manifold via a bakeable sapphire sealed leak valve. H_2O was obtained from a Millipore MilliQ system with a resistance of 18.2 MΩ/cm and placed in a glass bulb attached to the manifold and degassed by directly pumping on the volume of water. Gas doses were monitored with a Stanford Research Systems RGA-200 residual gas analyzer with a channeltron electron multiplier.

2.3. Speciation at high H_2O pressures studied by AP-XPS experiments at ALS

In order to help extrapolate the UHV information to atmospheric conditions, higher pressure experiments were performed using an ambient pressure XPS (AP-XPS) system to dose metallic and oxidized indium species with water. AP-XPS measurements were obtained at the Advanced Light Source at LBNL beamline 9.3.2. An In^0 sample was prepared from metallic indium shot, then Ar^+ sputtered at 2 keV and ~6 μA for 1.5 h, and an In_2O_3 sample was prepared by drop-casting isopropanol suspended powder onto a 1 micron film of Au on a 1 cm^2 Si wafer and then baking at 250 °C for 1 h. Ultra-high purity CO_2 (AirGas) and water from a Millipore MilliQ water system at 18.2 MΩ/cm was used after evacuating atmospheric gases with a mechanical pump. Gas pressures were monitored with a Stanford Research Systems RGA-100 residual gas analyzer in the electron analyzer chamber.

2.4. HREELS and TPD chamber and preparation

In an attempt to gather further information about the mechanism of indium oxidation and surface speciation distributions at oxidized indium surfaces, HREELS and TPD spectra were collected under UHV conditions from a flat, polycrystalline indium sample treated as described below. A custom chamber with a base pressure of 1.2×10^{-10} Torr was used to perform these HREELS and TPD measurements on an indium foil from Alfa Aesar (99.99% metals basis) mounted to a custom tantalum foil stage capable of being resistively heated and liquid N_2 cooled. The indium foil was brought to a mirror finish by pressing into a glass slide. An ELS 3000 HREELS system was used to obtain HREELS spectra and a Stanford Research Systems RGA-200 residual gas analyzer was used to record system pressure during TPD analysis. The sample was sputtered clean by backfilling the chamber with Ar to a pressure of 5×10^{-6} Torr and sputtering at 2 keV and ~6 μA for 1 h at an Ar^+ beam incidence angle of 20°.

HREELS spectra were obtained at the specular angle with a beam energy of 5 eV and direct transmission fwhm of ~3 meV, and incident beam angle of 60°.

TPD was performed with the sample 35° off normal from the RGA in an attempt to obtain a normalized desorption profile for various species. The stage was brought within 3 in. of the ionizing filament of the RGA. Programmed desorption was performed at a rate of 1 K/6 s.

3. Results and discussion

3.1. Authentic control samples

XPS of Ar^+ sputtered indium metal shows that sputtering removes almost all detectable O 1s and C 1s XPS signal after 1 h at 2 keV and 6 μA current to the sample. As seen in Fig. 1a, as the metallic In $3d_{5/2}$ peak at 443.7 eV is exposed, a significant plasmon loss feature grows in at 11.7 eV higher binding energy than its parent peak, in accordance with previous studies [11,13]. In addition, the full width half max (fwhm) of the In $3d_{5/2}$ and In $3d_{3/2}$ peaks are considerably less than the fwhm of the In 3d peaks of In_2O_3 (In $3d_{5/2}$ at 444.7 eV) and $In(OH)_3$ (In $3d_{5/2}$ at 445.1 eV), as seen in Fig. 1b and c, respectively. Even after sputtering at length, there is still a small O 1s signal from the indium substrate at 529.9 eV, which coincides with a small shoulder in the In 3d region with an In $3d_{5/2}$ peak at 444.8 eV. This O 1s signal likely is due to residual oxygen contamination in the chamber, which reacts before spectra can be obtained, or is from oxide already present in the indium sample.

As is common for the O 1s region previously reported for bulk In_2O_3 samples, there are two significant peaks present at 530.4 eV and 532.3 eV, generally attributed to bulk oxygen and surface adsorbed oxygen, respectively [11,13]. However, this assignment makes little sense when the peaks are of equal size, as is the case here. More likely,

Please cite this article as: Z.M. Detweiler, et al., The oxidation and surface speciation of indium and indium oxides exposed to atmospheric oxidants, Surf. Sci. (2015), http://dx.doi.org/10.1016/j.susc.2015.10.026

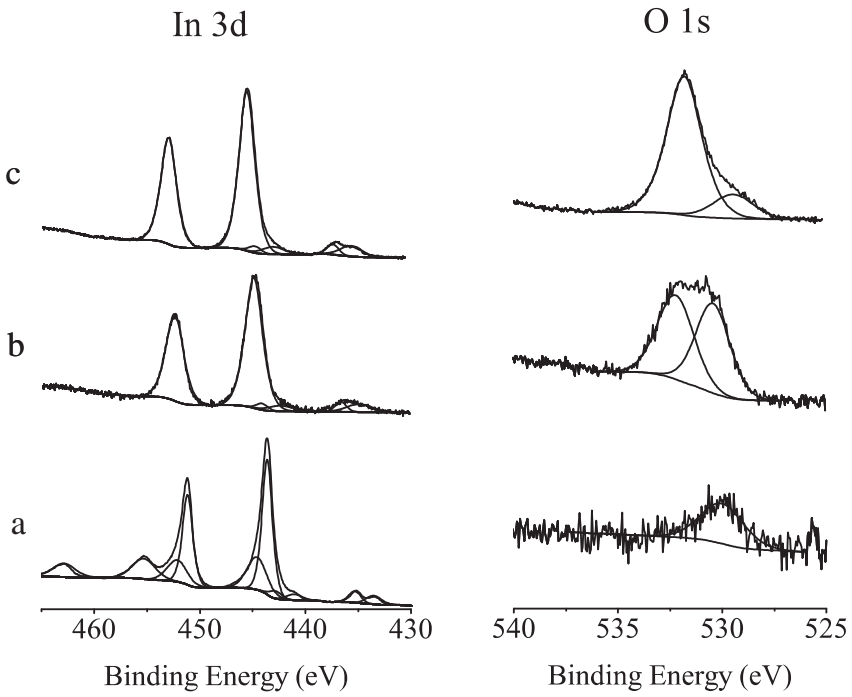

Fig. 1. XPS spectra of the In 3d and O 1s regions of (a) sputtered In metal, (b) In_2O_3, and (c) $In(OH)_3$.

the higher binding energy peak is actually a hydroxyl species [16,17]. The only other features seen in the In 3d region are due to $K\alpha_3$ and $K\alpha_4$ lines from the un-monochromated X-ray source, observed as satellites of large peaks at ~8.4 eV lower binding energy in collected XPS spectra.

The O 1s region of the $In(OH)_3$ sample demonstrates oxygen species which are similarly spaced as the In_2O_3 species, but shifted to slightly lower binding energy (529.3 eV and 531.7 eV, respectively). The shift in the In $3d_{5/2}$ peak to higher binding energy and shift in O 1s peaks to lower binding energy indicates that the In atom has lower electron density in $In(OH)_3$ than in In_2O_3, which is normally the case for metal hydroxides compared to their equivalent oxidation state metal oxide.

It is important to note that although the oxidized indium species are not metallic, In_2O_3 has a band gap of 2.3 eV and is commonly used with tin oxide as a transparent conducting film in electronics, and no significant charging was observed. $In(OH)_3$ on the other hand, displayed significant charging (up to 5 eV) and emitted a visible blue glow under X-ray illumination, understood to originate from oxygen vacancies in the crystal structure of the hydroxide [18].

3.2. Oxidation of indium with gases (O_2, H_2O and CO_2) monitored by XPS

After collecting peak information from the authentic samples, it was possible to begin measuring the change of indium surfaces during exposure to the small molecule oxidants of interest. As mentioned above, the presence of two oxygen species in In_2O_3 has been previously noted, but the assignment of the species that generates the higher binding energy O 1s peak at ~532 eV is not widely agreed upon, some assigning it to adsorbed oxygen and others attributing it to hydroxide. Those that attribute this O 1s species to adsorbed oxygen do so because they have only exposed the indium to oxygen in UHV conditions in order to monitor oxide growth, so that any oxygen signal was assumed to originate from O_2 [11,13]. Those who attribute the higher binding energy peak to a hydroxyl species do so in analogy to what has previously been reported for oxygen speciation at other metal oxide interfaces [17,19]. For this reason, the oxidation study performed by Rossnagel et al. at indium metal with gaseous oxidants was repeated, but with a focus on the O 1s speciation.

Fig. 2a again shows the Ar^+ sputtered indium substrate, which is essentially oxide free, demonstrated by the flat O 1s region. The In 3d region shows that there is a dominant In $3d_{5/2}$ peak at 443.7 eV with a strong 11.7 eV plasmon loss feature. The In LMM Auger region shows very sharp transitions, indicative of the metallic species, which is now dominant at the exposed interface. Fig. 2b shows the sputtered indium surface after it has been exposed to around 100,000 L of O_2. The O 1s region shows a large gain in O 1s signal, with a significant peak at 530 eV and a small shoulder around 531.8 eV. The In 3d region now distinctly shows two In $3d_{5/2}$ species, the metallic species at 443.7 and an oxidized species at 444.8 eV that matches closely with In_2O_3, but is not distinguishable, within the resolution of the spectrometer, from an $In(OH)_3$ In $3d_{5/2}$ signal. After oxygen exposure the In Auger region has significantly different, broadened features, with residual sharp peaks from the metallic species. XPS after exposing an equal amount of H_2O to the sputtered substrate is shown in Fig. 2c. The O 1s region demonstrates a significantly larger amount of the high binding energy oxygen species. In addition, the In 3d region shows a smaller amount of oxidation, which is also seen in the Auger region, where the metallic peaks are more pronounced in the region between the two indium species.

The oxidation of indium can be followed as a function of O_2 or H_2O exposure in order to determine sticking coefficients of the oxygen containing species and their oxidation rates of the bulk sample. Fig. 3 shows the In^{3+}/In^0 ratio, determined by comparing the peak areas for the two In $3d_{5/2}$ species at 444.8 eV and 443.7 eV, respectively. It is important to note that even though the sputtering has managed to dramatically rid the surface of oxidized indium, there is still a reasonable amount of oxidized indium peak area that cannot be removed. The ratios for indium speciation demonstrate similar behavior to that seen by Rossnagel et al., who reported the oxygen coverage as a function of O_2 and H_2O exposure [12].

For clarity in the following discussions, the main peaks of interest are summarized in Table 1. The In^{3+} peak is attributed to a mixed oxide state, including both indium oxide and indium hydroxide species. These two species cannot be resolved in the In 3d peak region with the photoelectron spectrometer used in this study. The O 1s peaks however, can be strongly attributed to the oxide speciation present. These

Please cite this article as: Z.M. Detweiler, et al., The oxidation and surface speciation of indium and indium oxides exposed to atmospheric oxidants, Surf. Sci. (2015), http://dx.doi.org/10.1016/j.susc.2015.10.026

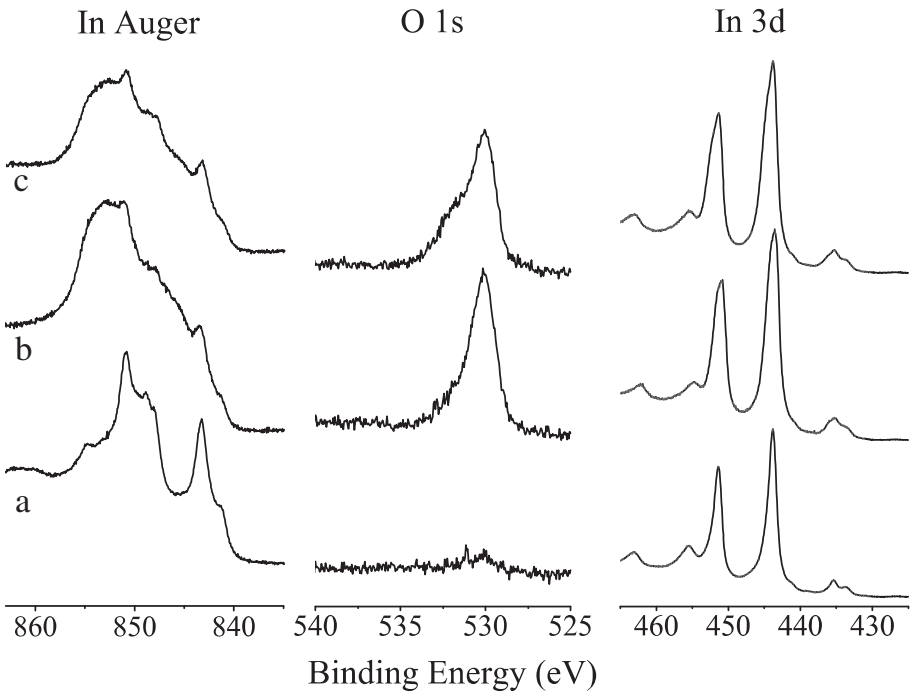

Fig. 2. XPS spectra of (a) an Ar^+ sputtered indium foil that has subsequently been exposed to (b) 100,000 L of O_2 or (c) 100,000 L of H_2O.

peak positions allow subsequent observations to be easily discussed and exposures will be presented in this context.

The In^{3+}/In^0 ratio for an O_2 exposed indium surface shows significant increase after about 20 L of oxygen exposure to the substrate. This ratio quickly increases over the next 1000 L of O_2 exposure, plateauing at around 5000 L. In contrast, the In^{3+}/In^0 ratio does not demonstrate significant oxidation until after 1000 L of H_2O exposure, and begins to plateau at around 100,000 L.

The most striking contrast between O_2 and H_2O oxidation of sputtered metallic indium foil in UHV is displayed in Fig. 4. By taking the ratio of O^{2-}/OH^- and plotting it against exposure for each oxidant, it becomes clear that the indium surface terminates differently in each case. The O^{2-} signal in the case of O_2 exposure is very large in the initial stages of oxidation and remains the dominant feature as exposure increases. The O^{2-}/OH^- ratio decreases logarithmically with O_2 exposure. The O^{2-}/OH^- ratio for H_2O oxidation of indium shows a much lower value at low water exposure values, and stays nearly constant until very high exposures.

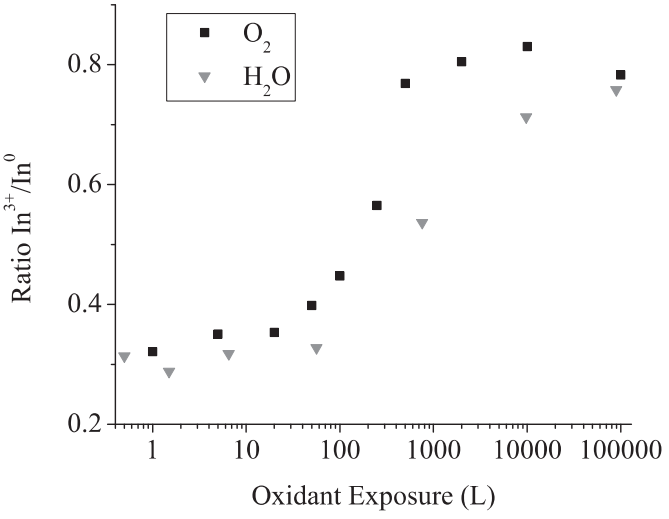

Fig. 3. In^{3+} (444.8 eV)/In^0 (443.7 eV) ratios plotted as a function of oxidant exposure by comparing the peak areas of the In $3d_{5/2}$ peaks at each exposure point.

This data suggests that O_2 is the better oxidant for indium and adsorbs dissociatively. Dissociation is likely driven by the oxidation of In^0 to In^{3+}, which starts to form an In_2O_3 layer. As more oxygen dissociatively adsorbs, O^{2-} is free to migrate to the oxide/metal interface growing a thin In_2O_3 film. As exposure increases, the O^{2-}/OH^- ratio decreases, suggesting that, slowly, due to trace H_2O or H_2 found in the chamber, OH^- is beginning to significantly coat the oxide film by water adsorption, potentially dissociating directly at an O^{2-} site into two OH^- in an acid–base equilibrium. The O^{2-}/OH^- ratio continues to decrease as both O^{2-} migration into the metallic phase slows, and trace H_2O and H_2 increasingly impinge or react on the surface.

Oxidation of In by H_2O takes place by a significantly different mechanism than O_2 oxidation, but yields a very similar oxide film. H_2O first adsorbs dissociatively, making surface hydroxide and hydride. Bulk oxidation occurs as surface hydroxide loses a proton to recombine with hydride, producing H_2, which desorbs, as observed and discussed in the TPD experiments below. The O^{2-} is then mobile enough to move to the In^0 interface below the exposed surface, creating an In_2O_3 under layer between the hydroxylated surface and the metallic bulk. It appears that the rate of oxidation slows as this oxide film grows. In the case of H_2O oxidation, the O^{2-}/OH^- ratio stays relatively constant as the oxidation occurs since there is an excess of OH^- at the surface that is constantly being replenished by incident water. As the oxide layer reaches saturation thickness for the P_{O_2} of the system, the OH^- signal becomes more intense as the driving force for incorporation of O^{2-} into the substrate decreases. The growth of oxide in both the H_2O and O_2 environments is in accord with the growth of an n-type semiconducting oxide, which agrees with previous reports on In_2O_3.

Table 1
Binding peak energies for the main indium 3d and oxygen 1s species highlighted in the following discussions.

	In 3d		O 1s	
	In^{3+}	In^0	O^{2-}	OH^-
Peak binding energy (eV)	444.8	443.7	530	532

Please cite this article as: Z.M. Detweiler, et al., The oxidation and surface speciation of indium and indium oxides exposed to atmospheric oxidants, Surf. Sci. (2015), http://dx.doi.org/10.1016/j.susc.2015.10.026

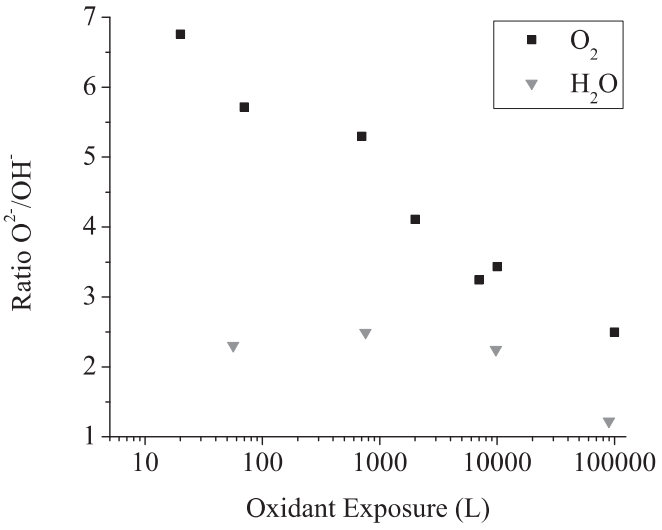

Fig. 4. The ratio of the low binding energy O 1s peak, associated with O^{2-}, and the high binding energy O 1s peak, associated with OH^-, plotted against the exposure of O_2 (black squares) and H_2O (gray triangles).

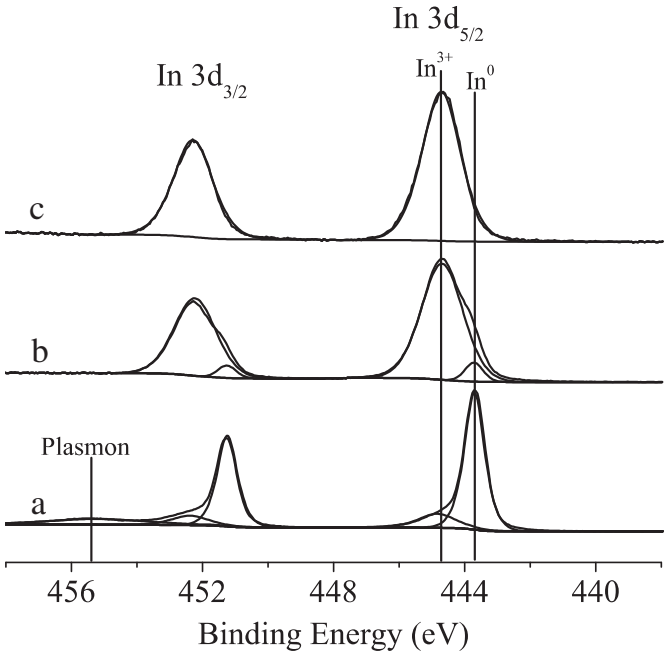

Fig. 5. AP-XPS spectra in the In 3d region for (a) an Ar^+ sputtered indium foil in UHV, (b) an Ar^+ sputtered indium foil while at a P_{H_2O} of 50 mTorr, and (c) In_2O_3 powder in UHV.

As was observed by Rossnagel et al., the present work does show slight oxidation of indium with CO_2 exposures. However, the exposures were so high and took so long that it is likely that trace O_2 and H_2O in the system may have been responsible for the oxidation [12]. The almost identical oxygen species observed for CO_2 exposure as for oxygen and water exposure supports the oxidation via trace O_2 and H_2O contamination. Small carbonate or potentially formate species were observed in the C 1s region at ~298 eV in all samples after significant exposure. This suggests that the sequestration of carbon as a carbonate or formate species is favorable, but highly surface localized. Due to the weak carbon peak intensity and the observation of this peak in samples not exposed directly to CO_2, it is difficult to confidently assign the origin of the carbon species as CO_2 or trace CO in the system.

3.3. Oxidation of indium with H_2O at ambient pressures

After having demonstrated that a significant exposure of oxidant causes the indium surface to reach a relatively constant oxide/hydroxide speciation, a stronger correlation to atmospherically exposed samples was desired. In order to obtain this link, the speciation of indium foil and indium oxide was observed with XPS at relatively high H_2O pressures. Fig. 5a shows the In 3d region of sputtered clean indium metal foil as acquired from a monochromatic X-ray source at the Lawrence Berkeley National Laboratory (LBNL) Advanced Light Source (ALS) Beamline 9.3.2 at 640 eV beam energy. The metallic In $3d_{5/2}$ peak at 443.7 eV is the main species, with a small, oxidized In $3d_{5/2}$ shoulder at a binding energy of 444.8 eV, in addition to corresponding In $3d_{3/2}$ peaks and plasmons at higher binding energies. Fig. 5b shows the Ar^+ sputtered foil at an ambient P_{H_2O} of 50 mTorr. The 444.8 eV peak becomes the dominant species under these conditions, and although the plasmon peak is no longer apparent, there is a distinct amount of metallic species still detectable. The In 3d region of an In_2O_3 powder, seen in Fig. 5c, did not change significantly between UHV and 50 mTorr P_{H_2O} conditions.

The ratio of In^{3+}/In^0 is 14.2 for the H_2O exposed foil, which is much higher than the In^{3+}/In^0 ratio observed in either O_2 or H_2O exposures of 100,000 L carried out at 10^{-5} Torr. This indicates that the observed plateaus of the In^{3+}/In^0 ratio in the O_2 and H_2O exposures under UHV/HV conditions were due to the limited extent of indium oxidation at low oxidant pressures.

As with the previous O_2 and H_2O exposures, more detail about surface speciation can be gleaned from the O 1s region of the spectrum. Fig. 6a shows the O 1s region of the Ar^+ sputtered indium foil, where there are small peaks that can be assigned to the O^{2-} and OH^- species. When the P_{H_2O} in the chamber is raised to 50 mTorr, both oxygen peaks increase in intensity dramatically, as seen in Fig. 6b, in unison with the In^{3+} peak seen Fig. 5b. The O^{2-}/OH^- ratio at 50 mTorr pressure of H_2O is 0.80, lower than previously observed in the UHV/HV exposures. Interestingly, as shown in Fig. 6c, the O^{2-}/OH^- ratio *increases* on evacuation of the H_2O to 0.82. This shows that the O^{2-}/OH^- ratio is dependent on the P_{H_2O} in the system, indicating that an equilibrium exists between the oxidized indium layer and $H_2O_{(g)}$.

Fig. 6d shows the O 1s region of an In_2O_3 powder, corresponding to the In 3d region shown in Fig. 5c. Both O 1s species are present with an

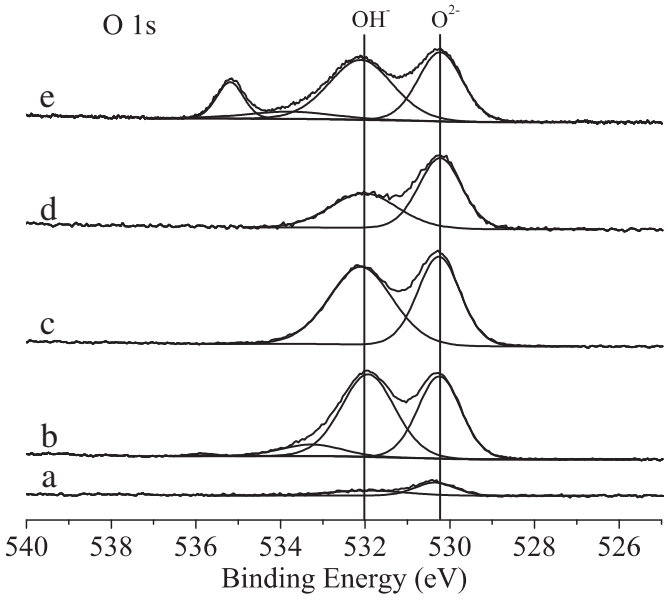

Fig. 6. AP-XPS spectra in the O 1s region for (a) an Ar^+ sputtered indium foil in UHV, (b) an Ar^+ sputtered indium foil while at a P_{H_2O} of 50 mTorr, (c) the foil after exposure at a P_{H_2O} of 50 mTorr after pumping back down to UHV pressure, (d) In_2O_3 powder in UHV and (e) while at a P_{H_2O} of 50 mTorr.

Please cite this article as: Z.M. Detweiler, et al., The oxidation and surface speciation of indium and indium oxides exposed to atmospheric oxidants, Surf. Sci. (2015), http://dx.doi.org/10.1016/j.susc.2015.10.026

O^{2-}/OH^{-} ratio of 1.32. Again, at a P_{H_2O} of 50 mTorr, the O^{2-}/OH^{-} ratio drops significantly to 0.74 as seen in Fig. 6e. The highest binding energy peak seen in Fig. 6b at 536 eV, and Fig. 6e at 535 eV is due to water in the vapor phase. It does not fall at the same binding energy in the two experiments because the sample of In_2O_3 charged significantly under the intense light source, and had to be calibrated according to the C 1s region. In both of these cases there is also a peak around 533.5 eV that can be attributed to physisorbed H_2O.

These combined UHV and ambient pressure XPS data demonstrate that the order and extent of indium oxidation is dictated by the distribution and pressure of oxidants present in the oxidizing atmosphere. The terminal hydroxylation of the indium substrate appears to depend on the level of water in this oxidizing atmosphere.

3.4. HREELS at metallic indium and oxidized indium with H_2O exposure

In order to probe the mechanism of adsorption and the potential implications on oxide growth and stability, HREELS was performed under UHV conditions to study the initial steps of metallic oxidation with O_2 and H_2O. HREELS spectra were obtained from an Ar^+ sputtered indium metal foil at 135 K, and are shown in Fig. 7a. Only after exposing to 40 L of H_2O were any H_2O vibrational modes observed. These modes were seen at 720 cm^{-1}, 1640 cm^{-1}, and 3660 cm^{-1}, which correspond to a frustrated rotation mode, a scissoring mode, and an O–H stretching mode of H_2O, respectively [20]. In addition to the H_2O vibrational modes, there also appears to be a mode at 450 cm^{-1}. This mode is likely an In–O mode of In hydroxide, as seen in previous work [21]. Additionally there are small hydrocarbon contamination modes seen at 1450 cm^{-1} and 2920 cm^{-1}. Exposing this surface to another 60 L of H_2O (total of 100 L) shows an increase in the water modes and the In–O mode, indicating both water ice and In hydroxide formation on the surface. If the sample is then annealed to 350 K (77 °C), the vibrational spectrum changes significantly, displaying a large peak at 530 cm^{-1} and a small OH stretch at 3620 cm^{-1}. The large peak around 530 cm^{-1} is most likely due to the formation of In oxide, and the small OH peak around 3600 cm^{-1} is due to small amounts of surface hydroxide formation by residual H_2O. Additionally, after annealing there is no detectable signal from molecular water vibrational modes.

The differences between water adsorption on indium oxide and metallic indium were observed by pre-oxidizing the metallic indium surface with oxygen and subsequently exposing water. Fig. 7b shows the Ar^+ sputtered surface after exposure to 50 L of O_2 at room temperature. The metal oxide mode seen after annealing the H_2O exposed metallic sample is seen again at 530 cm^{-1}. After exposing to a total of 2000 L of O_2, there is a very large peak at 560 cm^{-1}, and significant OH stretch mode 3610 cm^{-1}. There is, once again, hydrocarbon contamination present at 1450 and 2940 cm^{-1}. After collecting the 2000 L O_2 exposed HREELS spectrum, the sample was cooled to 135 K and then exposed to 10 L of H_2O. In this spectrum there were very strong H_2O vibrational modes observed at 1620 cm^{-1} and at 3580 cm^{-1}. Low energy water modes are obscured by a strong 560 cm^{-1} signal. This difference in OH stretch and bend frequency indicates formation of a more ordered ice film at the oxidized indium surface than at the metallic surface, perhaps due to the improved wetting of H_2O on the oxide surface compared to the metallic surface. Signal strength may also imply that there is more H_2O adsorbed on the oxide surface after 10 L of H_2O exposure than adsorbed to the metallic surface after 100 L of H_2O exposure. This could be explained by the formation of In hydroxide during the 100 L H_2O exposure.

The HREELS data strongly indicate that even at low temperatures, H_2O can dissociatively adsorb, but the formation of indium oxide is suppressed until higher temperatures. This may be due to the barrier to O^{2-} diffusion to the metallic interface through a growing oxide lattice thin film. From XPS and HREELS data, an indium surface appears to oxidize through the dissociative adsorption of O_2 or H_2O, followed by the diffusion of O^{2-} to the metal/oxide interface, forming a subsurface oxide film. The depth of this oxide and the speciation of the exposed surface is governed by the adjacent atmosphere composition.

3.5. TPD from metallic indium and oxidized indium in UHV after H_2O exposure

In order to further understand how H_2O adsorbs on indium metal and indium oxide differently and to observe what reaction products are present, water was exposed to the two substrates independently and then temperature programmed desorption spectra were obtained for varying surface exposures.

Fig. 8a demonstrates the desorption spectra following the exposure of 0.5 L, 1 L, 2 L, and 10 L of H_2O to an Ar^+ sputtered indium surface.

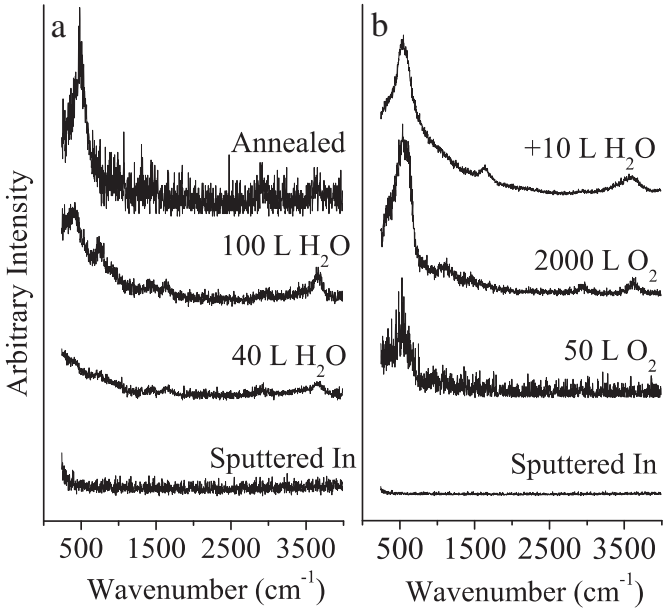

Fig. 7. HREELS spectra of (a) an Ar^+ sputtered metallic indium foil at ~135 K exposed to 40 L and 100 L of H_2O before annealing to 350 K, and (b) an Ar^+ sputtered metallic indium foil exposed to 50 L then 2000 L of O_2 at room temperature, before being cooled to ~135 K and then exposed to 10 L of H_2O.

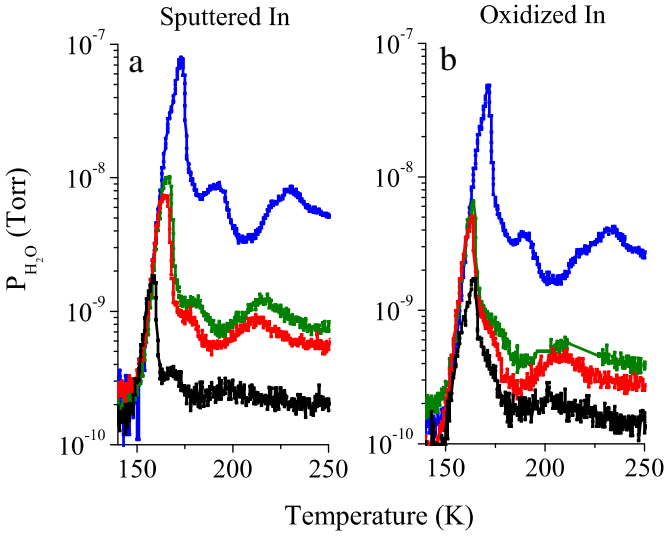

Fig. 8. TPD spectra on a logarithmic pressure scale of (a) sputtered indium and (b) indium exposed to 2000 L of O_2 at room temperature, each after being exposed to (black) 0.5 L, (red) 1 L, (green) 2 L, and (blue) 10 L of H_2O at ~135 K. (For interpretation of the references to color in this figure legend, the reader is referred to the web version of this article.)

Please cite this article as: Z.M. Detweiler, et al., The oxidation and surface speciation of indium and indium oxides exposed to atmospheric oxidants, Surf. Sci. (2015), http://dx.doi.org/10.1016/j.susc.2015.10.026

At 0.5 L of exposure, there are two distinct peaks at 158 K and 169 K, with a broad feature centered around 197 K. The TPD spectrum for 1 L of H_2O exposure shows similar peaks, but the peak positions shift to higher temperatures, 164 K, 176 K, and 212 K, respectively. H_2O exposure of 2 L shifts the peaks to even higher temperatures, 166 K, 181 K, and 216 K, respectively. Lastly, at 10 L of H_2O exposure on metallic indium, the desorption peaks shift to temperatures of 173 K, 191 K, and 230 K, respectively, with the broad peak at around 230 K distinctly displaying multiple features.

Fig. 8b shows the TPD spectra for the same H_2O exposures on an Ar^+ sputtered indium metal substrate that was exposed to ~2000 L of O_2 at room temperature to generate an oxidized surface. The 0.5 L H_2O exposure shows a distinctly different shape for the oxidized species, with two overlapping peaks. The primary peak is found at 163 K, with the shoulder centered at approximately 169 K, and a broad feature centered around 200 K. At 1 L H_2O exposure the primary peak area increases, but is centered at the same temperature as 0.5 L H_2O exposure: 163 K. The shoulder peak shifts to ~172 K, and the broad feature shifts to 208 K. After 2 L H_2O exposure the primary peak is still found at 163 K, with the shoulder shifted to ~175 K. The broad feature also appears to shift to higher temperature. Upon exposure to 10 L of H_2O, the primary peak shifts substantially to 171 K. The shoulder distinctly separates with a peak at 190 K, and the broad feature, similar to 10 L H_2O exposure on clean metallic indium, shows multiple desorption peaks centered at 233 K.

Fig. 9 shows the TPD for the low H_2O exposures from Fig. 8 on a linear scale instead of a logarithmic scale. Here the increase in peak area is more pronounced and the peak position shifts are emphasized. The behavior of the primary peak in Fig. 9a is indicative of a zeroth order process, which is typical of molecular water adsorption to form ice. This indicates that the adsorbed water at this temperature is more strongly interacting with itself than with the metallic substrate [22]. The dramatic change in peak shape and position to higher temperatures in the primary peak for the oxidized indium, seen in Fig. 9b, is indicative of a change in desorption to first order [23]. The higher desorption temperature observed for low H_2O exposure indicates greater adsorption strength between H_2O and the oxidized substrate than between H_2O and the metallic substrate. The change to first order reaction is indicative of a non-dissociative adsorption of H_2O on the oxidized substrate [24].

In addition to monitoring H_2O (18 M/Z) during programmed desorption, O_2 (32 M/Z), H_2 (2 M/Z), N_2 (28 and 14 M/Z), CO (28 and 12 M/Z) and Ar (40 M/Z) were also recorded. Of these, only H_2 showed significant desorption over the observed temperature range. The single H_2 peak corresponded closely to desorption of the primary H_2O peak for both metallic indium and oxidized indium, and sat on a higher baseline than the other monitored gases. Overlaid H_2 and H_2O TPD spectra for 1 L of H_2O exposure on metallic indium, Fig. 10a, and oxidized indium, Fig. 10b, show similar relative H_2/H_2O peak ratios. Interestingly, the H_2 peak and H_2O peak from the oxidized indium sample appear at the same temperature, 163 K. This is not the case for H_2 and H_2O desorption from metallic indium, where H_2O peaks at 164 K, while H_2 peaks slightly later, at 166 K, which corresponds to a delay of ~15 s at this heating rate. This offset in H_2 peak from the H_2O primary peak is observed at 2 L H_2O exposure to metallic indium as well, while H_2 and H_2O peaks for the 2 L H_2O exposure on oxidized indium again demonstrate coincidence.

The TPD spectra suggest that H_2O adsorbs more strongly on the oxidized surface, where the adsorption of H_2O to the metal surface at these temperatures is a weaker interaction. Further, the metallic indium demonstrates a slightly higher temperature release of H_2, suggesting that as the substrate desorbs water, at some small coverage, the metallic substrate is oxidized. This is supported by the change in HREELS spectrum after annealing the substrate above the desorption peak temperature, as seen in Fig. 7, showing the presence of metal-oxide after water is desorbed.

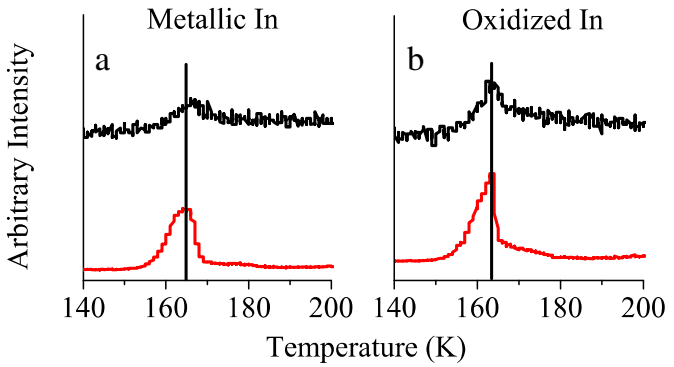

Fig. 10. TPD spectra on a linear pressure scale of (red) H_2O and (black) H_2 desorption from (a) Ar^+ sputtered metallic indium, and (b) 2000 L O_2 oxidized indium. (For interpretation of the references to color in this figure legend, the reader is referred to the web version of this article.)

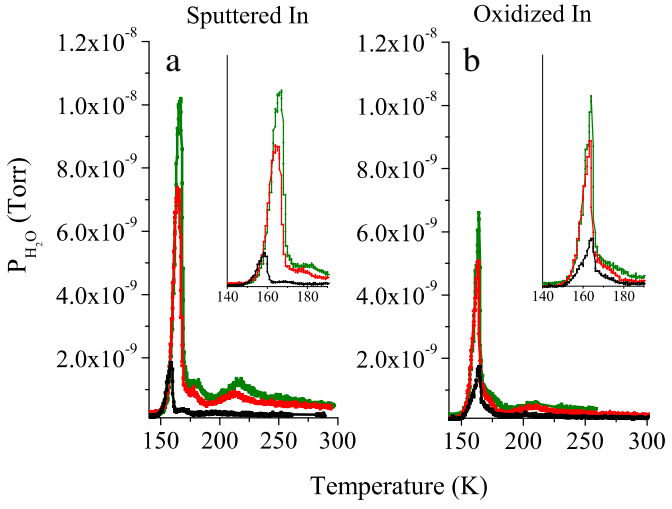

Fig. 9. TPD spectra on a linear pressure scale of (a) sputtered indium and (b) indium exposed to 2000 L of O_2 at room temperature, each after being exposed to (black) 0.5 L, (red) 1 L, and (green) 2 L of H_2O at ~135 K. The inset for each spectrum shows the primary peak region in greater detail. (For interpretation of the references to color in this figure legend, the reader is referred to the web version of this article.)

4. Conclusions

From the data discussed above, it is evident that the major species exposed at a native indium metal surface under atmospheric conditions is a hydroxide species. O_2 and H_2O exposure demonstrates that after or during terminal hydroxylation, an In_2O_3 layer is formed. The hydroxyl termination of this native oxide is also observed in pure In_2O_3 samples, attesting to the basicity of the metal oxide, which forms OH groups from oxide and H_2O. There is a strong possibility that the equilibrium that favors hydroxyl formation at high H_2O pressures acts to passivate the metal from further oxidation in a manner similar to other group XIII elements [25]. The data demonstrate how a humid atmosphere can directly affect the order of oxidation and the potential for processing conditions to significantly impact the conductivity of the final oxide due to incorporation of hydroxide doping. This understanding is useful for the development of further indium-derived products. This work also has potential implications for the mechanistic pathways of indium surface catalyzed reactions currently being performed in various settings. It is thus important that the active environment be considered in indium catalysis and indium materials synthesis, since the surface speciation is a sensitive function of the composition of the oxidizing atmosphere.

Please cite this article as: Z.M. Detweiler, et al., The oxidation and surface speciation of indium and indium oxides exposed to atmospheric oxidants, Surf. Sci. (2015), http://dx.doi.org/10.1016/j.susc.2015.10.026

Acknowledgments

This work was partially supported by the US National Science Foundation, Division of Chemistry, CHE-1213216 (SLB), and CHE-1308652 (ABB). Support of an Advanced Light Source beam time award is also acknowledged. The Advanced Light Source is supported by the Director, Office of Science, Office of Basic Energy Sciences, of the U.S. Department of Energy under Contract No. DE-AC02-05CH11231.

References

[1] Blackie Academic & Professional, London, 1993.
[2] G.D. Bennett, L.A. Paquette, Org. Synth. 77 (2000) 107.
[3] A. Wildermann, Y. Foricher, T. Netscher, W. Bonrath, Pure Appl. Chem. 79 (2007) 1839.
[4] K.L. Purvis, G. Lu, J. Schwartz, S.L. Bernasek, J. Am. Chem. Soc. 122 (8) (2000) 1808.
[5] Y. Ueda, J. Abe, H. Murata, Y. Gotoh, O. Sakai, Jpn. J. Appl. Phys. 53 (3S2) (2014) 03DG03.
[6] R. Schlaf, H. Murata, Z.H. Kafafi, J. Electron Spectrosc. Relat. Phenom. 120 (1–3) (2001) 149.
[7] T. Krishnakumar, R. Jayaprakash, V.N. Singh, B.R. Mehta, A.R. Phani, J. Nano. Res. 4 (2008) 91.
[8] Z.M. Detweiler, J.L. White, S.L. Bernasek, A.B. Bocarsly, Langmuir 30 (25) (2014) 7593.
[9] S.J. Splinter, N.S. McIntyre, W.N. Lennard, K. Griffiths, G. Palumbo, Surf. Sci. 292 (1,Äi2) (1993) 130.
[10] A.P. Grosvenor, B.A. Kobe, N.S. McIntyre, Surf. Sci. 565 (2–3) (2004) 151.
[11] A.W.C. Lin, N.R. Armstrong, T. Kuwana, Anal. Chem. 49 (8) (1977) 1228.
[12] S.M. Rossnagel, H.F. Dylla, S.A. Cohen, J. Vac. Sci. Technol. 16 (2) (1979) 558.
[13] R.W. Hewitt, N. Winograd, J. Appl. Phys. 51 (1980) 2620.
[14] P. Sen, M.S. Hegde, C.N.R. Rao, Appl. Surf. Sci. 10 (1) (1982) 63.
[15] J.I. Jeong, J.H. Moon, J.H. Hong, J.Ä. Kang, Y. Fukuda, Y.P. Lee, J. Vac. Sci. Technol. A 14 (2) (1996) 293.
[16] J.-C. Dupin, D. Gonbeau, P. Vinatier, A. Levasseur, Phys. Chem. Chem. Phys. 2 (6) (2000) 1319.
[17] S. Kleber, M.J. Graham, S. Moisa, G.I. Sproule, X. Wu, D. Landheer, A.J. SpringThorpe, P.J. Barrios, P. Schmuki, in: P. Marcus, V. Maurice (Eds.), Passivation of Metals and Semiconductors, and Properties of Thin Oxide Layers: A Selection of Papers from the 9th International Symposium, Paris, France, 27 June–July 2005, Elsevier B. V., Amsterdam 2006, p. 263.
[18] C. Li, S. Lian, Y. Liu, S. Liu, Z. Kang, Mater. Res. Bull. 45 (2) (2010) 109.
[19] M. Faur, M. Faur, D.T. Jayne, M. Goradia, C. Goradia, Surf. Interface Anal. 15 (11) (1990) 641.
[20] D.V. Chakarov, L. Österlund, B. Kasemo, Vacuum 46 (8–10) (1995) 1109.
[21] T. Yan, J. Long, Y. Chen, X. Wang, D. Li, X. Fu, C. R. Chim. 11 (1–2) (2008) 101.
[22] W. Rudzinski, W.A. Steele, G. Zgrablich, Equilibria and Dynamics of Gas Adsorption on Heterogeneous Solid Surfaces, Elsevier, 1997.
[23] J.W. Niemantsverdriet, K. Markert, K. Wandelt, Appl. Surf. Sci. 31 (2) (1988) 211.
[24] K.W. Kolasinski, Surface Science: Foundations of Catalysis and Nanoscience, 3rd ed. Wiley, 2012.
[25] J. van den Brand, P.C. Snijders, W.G. Sloof, H. Terryn, J.H.W. de Wit, J. Phys. Chem. B 108 (19) (2004) 6017.

Please cite this article as: Z.M. Detweiler, et al., The oxidation and surface speciation of indium and indium oxides exposed to atmospheric oxidants, Surf. Sci. (2015), http://dx.doi.org/10.1016/j.susc.2015.10.026